

# Modeling of the effective field dependent mobility for TCAD simulation of DRAM cell transistors considering the random discrete dopants

Daewon Kim, Hoin Yu, Seungman Rhee and Young June Park

Department of Electrical and Computer Engineering, Seoul National University

1 Gwanak-ro, Gwanak-gu, Seoul, Republic of Korea

E-mail: zephyr9@snu.ac.kr, ypark@snu.ac.kr

**Abstract**—A new effective field dependent mobility model for the TCAD simulation considering the random discrete dopants is presented. When the devices with the random discrete dopants are simulated, the conventional mobility models designed for the continuous doping devices result in abnormally high currents, since the intrinsic region in the vicinity of the single dopants has unreasonably high mobility. The proposed mobility model suggests that the value of mobility in the specific mesh depends on the ‘effective field’ defined by the carrier concentration of the mesh, not the doping concentration. With the set of proper fitting parameters, the model can be adopted as a general mobility modeling considering the random dopants. As an example, the model is applied to predict the current variability due to the effect of the random discrete dopants in the source and drain overlap region of modern DRAM cell transistors.

**Keywords**—mobility; effective field; TCAD simulation; DRAM cell transistors; random discrete dopants; current variability

## I. INTRODUCTION

As the MOSFET technology is scaled down to sub-100 nm nodes, the impurity doping by ion-implantation shows inevitable randomness and discreteness. Most of the researches on the effect of the random discrete dopants (RDD) have been focused on the electrostatic effect in the channel region to predict the variability of the threshold voltage. However, in the scaled devices after 20 nm technology nodes, the RDD effects in the source/drain (S/D) regions become significant. The effect is more important in the state-of-the-art dynamic random-access memory (DRAM), where the impurity doping of the S/D regions is lower than the conventional devices because the gate-induced drain leakage current should be minimized in order to maintain the electric charges in storage capacitors as long as possible [1].

The statistical impacts caused by the RDD effects in the S/D regions of the extremely small devices such as the current variation are as important as the threshold voltage variation caused by the RDD effects in the channel region. The electrostatic and its quantum correction dealing with the RDD and its statistical impacts have been dealt with, for example, the density gradient quantum model [2]. However, the mobility model including the impurity scattering to account for the RDD effect has not been fully exploited even though the model is critically important to predict the current and its variation [3,4].

In this paper, we propose a new ‘ $E_{eff}$ ’ dependent mobility model for the TCAD simulation, where  $E_{eff}$  is a new parameter depending on the carrier concentration of the corresponding mesh. In the following sections, the development of the model based on  $E_{eff}$  and its application to the prediction of the current variation associated with the S/D overlapping region of modern DRAM cell transistors will be shown.

## II. EFFECTIVE FIELD DEPENDENT MOBILITY MODEL

In the proposed mobility model, we define the effective field  $E_{eff}(\mathbf{r})$  in a mesh as

$$E_{eff}(\mathbf{r}) = wqn(\mathbf{r}) / \epsilon_s, \quad (1)$$

where  $\mathbf{r}$  is the position vector of each meshes,  $n(\mathbf{r})$  is the carrier concentration,  $w$  is the mesh spacing for unit conversion from volumetric carrier concentration to areal one and  $q$  is the elementary charge constant. To determine  $n(\mathbf{r})$ , we used the density gradient method to include the quantum effects caused by the surface potential [2] or the discrete dopants [5] as,

$$n(\mathbf{r}) = N_C F_{1/2}((E_F - E_C + q\Lambda) / k_B T), \quad (2)$$

where  $F_{1/2}(\eta)$  is the Fermi-Dirac integral of order 1/2,  $\Lambda$  is the quantum correction term from the density gradient method derived as [2]

$$\Lambda = (\hbar^2 / 6m^*) (\nabla^2 \sqrt{n} / \sqrt{n}). \quad (3)$$

Using the effective field defined in (1), the low-field mobility model has been set up in two steps; firstly, the bulk mobility model is expressed as,

$$\mu_{bulk}(\mathbf{r}) = F(B/E_{eff}^\beta + C/E_{eff}^\gamma + D/E_{eff}^\delta), \quad (4)$$

and secondly, the surface mobility model is added as,

$$\mu_{low}(\mathbf{r}) = (G \exp(-x/l_{crit}) + 1) \mu_{bulk}(\mathbf{r}), \quad (5)$$

where  $x$  is the normal distance from the silicon-gate dielectric interface. The fitting parameters  $\{B, C, D, \beta, \gamma, \delta, F, G, I_{crit}\}$  in the above two equations are found by fitting to the Masetti model for the continuously doped bulk, followed by fitting to the accumulation layer mobility model for the surface mobility [6,7]. Similar procedure can be applied to find the inversion layer mobility model. The fitting procedure from the actual discrete doping to the equivalent doping concentration assuming the continuous doping will be explained in Sec. III in detail.

### III. MODEL PARAMETERS

In order to determine the fitting parameters in (4) and (5), we implemented two test structures sequentially as shown in Fig. 1(a) and (b); (A) N-type resistor bars with uniform doping distribution of specific concentrations, (B) the same as (A) but with the gated structure with the gate having the mid-gap Fermi level as in the typical modern DRAM cell transistors [1]. Furthermore, the same structures but with the gradual doping distribution from  $10^{20} \text{ cm}^{-3}$  to  $10^{17} \text{ cm}^{-3}$  have been simulated in order to verify that the derived fitting parameters from the uniform doping are also valid on the general nonuniform doping cases.

The doping distributions of the simulating structures have been implemented by two versions as shown in Fig. 1: First one has continuous doping and there are no meshes containing the intrinsic concentration. On the other hand, another one is the group of multiple samples with RDD having the average doping concentration same as the continuous counterpart. In this case, there are meshes with extremely high doping concentration ( $10^{21} \text{ cm}^{-3}$  in 1 nm mesh) surrounded by the intrinsic meshes. For an example, the gradually doped resistor from  $10^{20} \text{ cm}^{-3}$  (top) to  $10^{17} \text{ cm}^{-3}$  (bottom) contains most of randomly distributed single dopants at the top, and numbers of dopants become scarce to the bottom as shown in Fig. 1(d).

We obtained the fitting parameters in (4) and (5) by fitting the average current of the multiple samples, which have various spatial distribution of dopants. The parameters reproduce the current of the continuous doping counterpart with the conventional mobility models, e.g., the Masetti and the accumulation layer mobility model.

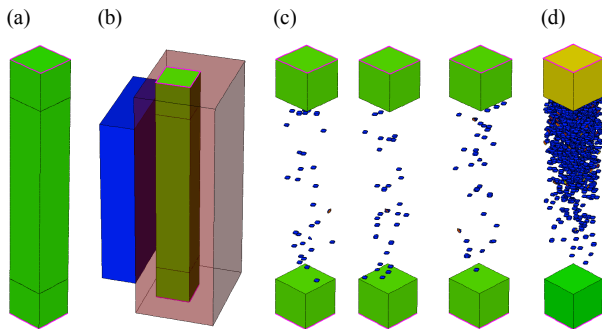


Fig. 1. The structures to determine and verify the fitting parameters. (a) The N-type resistor for  $\mu_{bulk}(\mathbf{r})$  in (4). (b) The gated resistor for  $\mu_{low}(\mathbf{r})$  in (5). (c) A group of RDD samples with different spatial distributions of dopants. (d) A nonuniform RDD sample with gradual doping concentration from  $10^{20} \text{ cm}^{-3}$  to  $10^{17} \text{ cm}^{-3}$ .

The applied voltages for the fitting procedure are the  $V_{ds}$  of 20 mV and  $V_{gs}$  of 3 V, respectively. All the simulations have been performed using the Sentaurus tool [8].

#### A. Resistor bars for the bulk mobility

For the fitting parameters of  $\mu_{bulk}(\mathbf{r})$  in (4), we consider the uniformly doped resistors of  $20 \times 20 \times 140 \text{ nm}$  with concentration of  $10^{17} \text{ cm}^{-3}$  through  $10^{20} \text{ cm}^{-3}$ . As shown in Fig. 2, within the length of 140 nm, only the dopants in the intermediate part of 100 nm have been distributed randomly on the intrinsic base, but both edges of 20 nm have continuous doping concentration in order to create Ohmic contacts at each ends of resistor bars.

The RDD samples are selected such that the number of discrete dopants is the same with the effective number of dopants in the continuous counterparts. For example, since the continuous counterpart of  $10^{17} \text{ cm}^{-3}$  has 4 dopants effectively in the volume of  $20 \times 20 \times 100 \text{ nm}$ , only the samples containing 4 discrete dopants are selected. In this way, we are convinced that any current deviation between RDD samples and their continuous counterparts is the matter of the mobility models, not the number of total carrier numbers.

After determination of the fitting parameters in (4), the bulk mobility model  $\mu_{bulk}(\mathbf{r})$  is tested on the resistor with the gradual doping concentration from  $10^{20} \text{ cm}^{-3}$  (top) to  $10^{17} \text{ cm}^{-3}$  (bottom), as shown in Fig. 1(d).

#### B. Gated resistor for the surface mobility

Secondly, in order to determine the fitting parameters of  $\mu_{low}(\mathbf{r})$  in (5), we repeated the same procedure in Sec. III-A on the gated resistor structures which have doping concentration of  $10^{17} \text{ cm}^{-3}$  through  $10^{20} \text{ cm}^{-3}$ .

### IV. APPLICATION TO THE DRAM STRUCTURE AND DISCUSSIONS

Using the mobility model with the parameters summarized in Table I and Fig. 3, we simulated the specific structure, which can be considered to the simplified S/D overlapping region which is partially extracted from the modern DRAM cell transistors [1] as shown in Fig. 4. This structure is constructed with the  $20 \times 20 \times 140 \text{ nm}$  N-type resistor with gradual doping concentration from  $10^{20} \text{ cm}^{-3}$  (top) to  $10^{17} \text{ cm}^{-3}$  (bottom), one-sided vertical gate and 60 Å of gate dielectric. The vertical gate

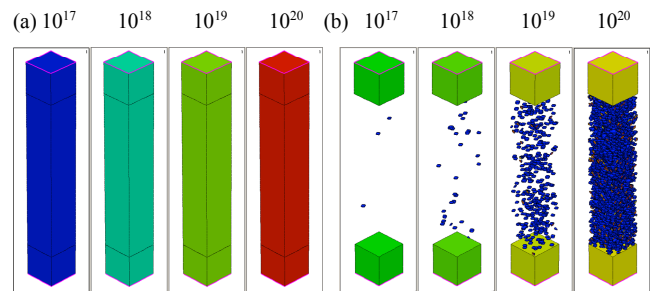


Fig. 2. The N-type resistor bars with uniform dopings of  $10^{17} \text{ cm}^{-3}$  through  $10^{20} \text{ cm}^{-3}$ . (a) We have set the currents of the continuous dopings with the conventional mobility models as the target. (b) The generation from the continuous doping of (a), but only the samples containing the same number of dopants with their continuous counterparts are selected.

is partially attached at the lower side of the resistor, and silicon nitride ( $\text{Si}_3\text{N}_4$ ) is located at the upper side to simulate the capping material. As a result, the average current of the samples with RDD is matched to the current of the continuous counterpart, as shown in Fig. 5

In the mobility contour plots in Fig. 6 for the gradual doping samples with the partial gated structure, we can observe three important features as follows:

- The meshes of the intrinsic concentration have abnormally high mobility if the mobility models for the continuous doping concentration are employed in the RDD samples as in Fig. 6(b) and Fig. 7(a). This can explain why the abnormally higher current is obtained when the conventional mobility models are employed in the RDD samples as in Fig. 8. However, since the carrier concentration  $n(r)$  is nonzero even in meshes with no dopants by the proper electrostatic model such

as the density gradient method, the effective field  $E_{eff}(r)$  and the corresponding mobility  $\mu_{low}(r)$  can have appropriate values, as in Fig. 6(c) and Fig. 7(b).

- Using the conventional mobility models, especially the doping-dependent model such as Masetti model, any meshes with the same doping concentration result in the same values of mobility uniquely. Meanwhile, since the carrier concentrations  $n(r)$  of the same intrinsic meshes are automatically diverse due to the spatial distribution of neighboring dopants, the resultant mobility  $\mu_{bulk}(r)$  can be calculated differently. This phenomenon implies the nonlocal property of the mobility in the vicinity of the RDD, and also reflects the screening effect by the mobile carriers.
- For the mobility near the silicon-gate dielectric interface, the value of the effective field dependent mobility

TABLE I. DETERMINED SET OF THE FITTING PARAMETERS

Param.	$B$	$C$	$D$	$\beta$	$\gamma$
Value	0.0022	0.098	21.7	-0.125	0.422
Param.	$\delta$	$F$	$G$	$l_{crit}$	
Value	0.411	1195	1.541	8.6E-8	

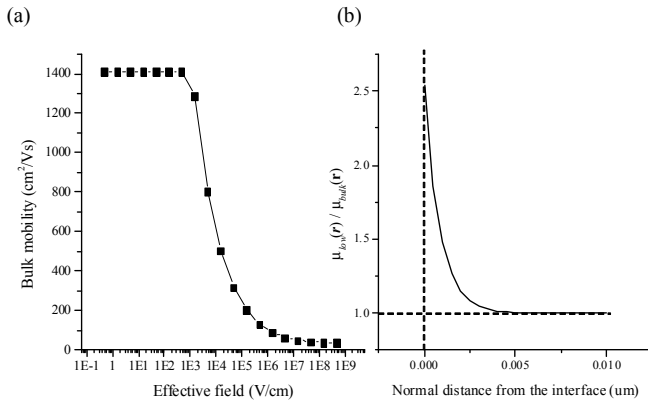


Fig. 3. (a) The bulk mobility vs. the effective field. Using the set of fitting parameters in Table I, the effective field  $10^5$  V/cm is related to approximately  $10^{18}$   $\text{cm}^{-3}$  of the electron density. (b) The ratio of  $\mu_{low}(r)$  to  $\mu_{bulk}(r)$  in (5) is plotted by the normal distance  $x$  from the silicon-gate dielectric interface.

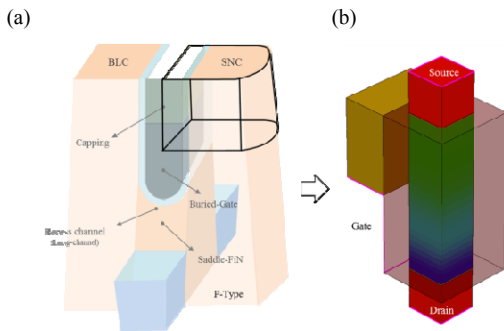


Fig. 4. (a) The schematic of the modern DRAM cell transistors with the vertical gate and the fin channel. (b) The simplified structure of the S/D overlapping region which reflects the part marked by the black boundary line in (a) for the TCAD simulation.

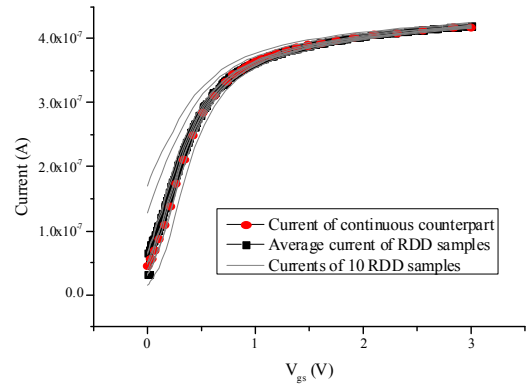


Fig. 5. The  $I_d$ - $V_g$  curve of the average current of RDD samples and the current of the continuous counterpart in the gated resistor with gradual doping.

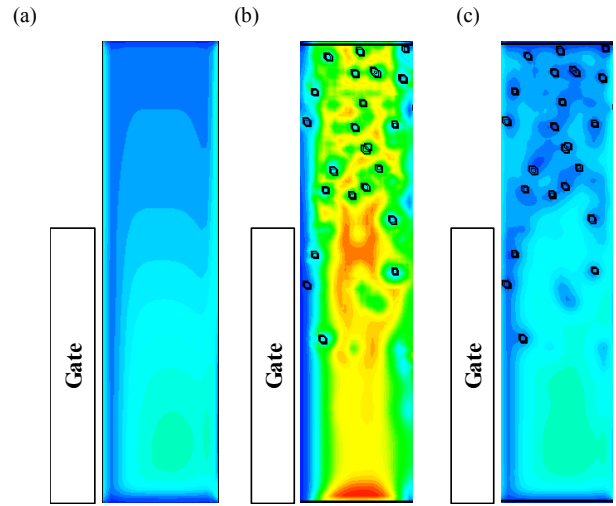


Fig. 6. The mobility contour plot on the cutplane of the silicon region. Black dots indicate the meshes including the discrete dopant. The mobility range of the plot is varied from  $1400 \text{ cm}^2/\text{Vs}$  (red) to  $20 \text{ cm}^2/\text{Vs}$  (blue) (a) Continuous doping with the conventional mobility models. (b) An RDD sample using the conventional mobility models (c) The same sample with (b), but using the proposed mobility model. The range of color indicates the range of mobility is similar to the continuous counterpart of (a).

should be boosted about 2.5 times, which can be derived from the value of  $G+1$  with  $x=0$  in the exponential term of (5). Also, the effective distance by the surface mobility is approximately 3 nm from the interface. From this observation, we can infer the impurity scattering is quite stronger than the surface scattering at the equivalent effective field.

Finally, as another application of the mobility model, we have simulated the gated resistor at  $V_{gs}$  of 3 V and  $V_{ds}$  of 1.2 V, which is actual operation voltage of the typical DRAM cell transistors. After modifying the coefficient of the velocity saturation model using the methodology of [9], we have obtained that the coefficient of variation (CV) of the current in the S/D overlap region is 2.9%, which cannot be neglected in the actual DRAM operations. In the state-of-the-art DRAM cell transistors, the overall CV of the current is roughly 4-5%. Therefore, if one can suppress the RDD effects in the S/D overlap region, the overall variation will be diminished since the two CV values are comparable.

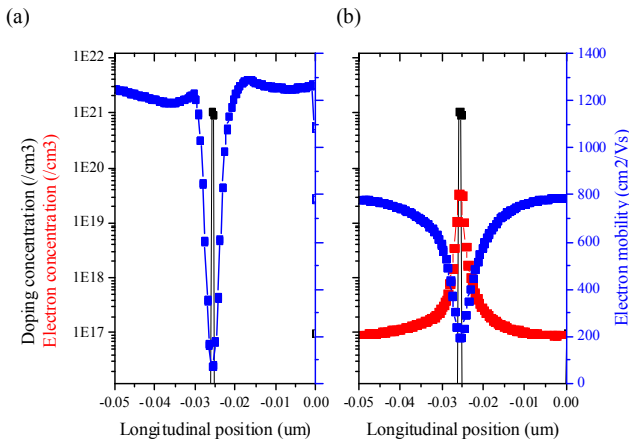


Fig. 7. The mobility plot in the vicinity of a discrete dopant located on the intrinsic silicon base. (a) If the electron mobility depends on the doping concentration directly by the Masetti model, only the mesh with a dopant has the minimum mobility and the rest meshes have maximum values. (b) In the proposed model, the mobility depends on the effective field which is defined by the electron density. Using a proper electrostatic method, the electron density is distributed smoothly near the dopant without unphysical trapping.

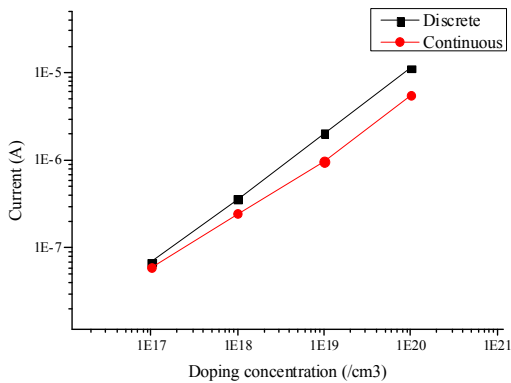


Fig. 8. The simulated current vs. the doping concentration of the uniformly doped resistors. The conventional mobility model is applied in both cases without care.

## V. CONCLUSIONS

We have proposed a new mobility model for the random discrete dopants (RDD) based on a new parameter,  $E_{eff}$ . In the suggested model, the mobility value of the specific mesh point depends on the effective field defined by the carrier concentration of the mesh. By choosing a proper electrostatic model such as the density gradient method, the effective field and the corresponding mobility may contain a proper treatment of the quantum mechanical correction. By applying the proposed model to the N-type silicon resistors and the gated resistors, we have successfully reproduced the current of the continuously doped structures with the conventional mobility models. The model has been applied to the source-drain (S/D) and gate overlapping region in the modern DRAM cell transistors. The current variation of DRAM cell transistors due to the RDD effects is anticipated 2.9%, which is comparable to the overall current variation of the modern DRAM cell transistors.

## REFERENCES

- [1] J. M. Park, Y. S. Hwang, S.-W. Kim, S. Y. Han, J. S. Park *et al.*, "20nm DRAM: A new beginning of another revolution," 2015 IEEE Int. Elec. Dev. Meeting (IEDM), Washington, DC, 2015, pp. 26.5.1-26.5.4.
- [2] M. G. Ancona and G. J. Iafrate, "Quantum correction to the equation of state of an electron gas in a semiconductor," *Phys. Rev. B*, vol. 39, no. 13, pp. 9536-9540, 1989.
- [3] A. Asenov, F. Adamu-Lema, X. Wang, and S. M. Amoroso, "Problems with the continuous doping TCAD simulations of decananometer CMOS transistors," *IEEE Trans. Electron Devices*, vol. 61, no. 8, pp. 2745-2751, 2014.
- [4] S. M. Amoroso, F. Adamu-Lema, A. R. Brown, and A. Asenov, "A mobility correction approach for overcoming artifacts in atomistic drift-diffusion simulation of nano-MOSFETs," *IEEE Trans. Electron Devices*, vol. 62, no. 6, pp. 2056-2060, 2015.
- [5] A. R. Brown, J. R. Watling, G. Roy, C. Riddet, C. L. Alexander *et al.*, "Use of density gradient quantum corrections in the simulation of statistical variability in MOSFETs," *J. Comput. Electron.*, vol. 9, no. 3-4, pp. 187-196, 2010.
- [6] G. Masetti, M. Severi, and S. Solmi, "Modeling of carrier mobility against carrier concentration in arsenic-, phosphorus-, and boron-doped silicon," *IEEE Trans. Electron Devices*, vol. 30, no. 7, pp. 764-769, 1983.
- [7] S. A. Mujtaba, "Advanced mobility models for design and simulation of deep submicrometer MOSFETs," Ph.D. thesis, 1995.
- [8] Sentaurus™ user guide, version L-2016.03, 2016.
- [9] H. Yu, S. Choi, D. Kim, S. Rhee and Y. J. Park, "A Mobility model for random discrete dopants and its impact on the current drivability of DRAM cell," unpublished.